Molecular Pharmacology Fast Forward. Published on August 23, 2019 as DOI: 10.1124/mol.119.117432
This article has not been copyedited and formatted. The final version may differ from this version.

Arylamine N-acetyltransferase 1 regulates expression of matrix metalloproteinase 9 in breast cancer cells: role of HIF1-α

Pengcheng Li, Neville J. Butcher and Rodney F. Minchin

School of Biomedical Sciences, University of Queensland, St Lucia, Australia

Molecular Pharmacology Fast Forward. Published on August 23, 2019 as DOI: 10.1124/mol.119.117432
This article has not been copyedited and formatted. The final version may differ from this version.

Running title: NAT1 regulates MMP9

Corresponding author:

Dr NJ Butcher,

School of Biomedical Sciences,

University of Queensland, St Lucia, QLD 4072, Australia.

Tel: 64-7-3365-2684,

Fax: 64-7-3365-1766,

E-mail: n.butcher@uq.edu.au

Number of Pages: 25

Number of Tables: 2

Number of Figures: 5

Number of References: 38

Number of words in Abstract: 176

Number of words in Introduction: 470

Number of words in Discussion: 62

ABBREVIATIONS: AP-1, activator protein 1; HIF1-α, hypoxia-inducible factor 1-alpha; MMP, matrix metalloproteinase; NAT1, arylamine N-acetyltransferase 1; SMYD3, SET and MYND-domain containing 3

ABSTRACT

Arylamine N-acetyltransferase 1 (NAT1) is a drug metabolizing enzyme that influences cancer cell proliferation and survival. However, the mechanism for these effects is unknown. Because of previous observations that NAT1 inhibition decreases invasiveness, we investigated the expression of the metalloproteinase MMP9 in human breast cancer samples and in cancer cells. We found a negative correlation between the expression of NAT1 and MMP9 in 1904 breast cancer samples. Moreover, when NAT1 was deleted in highly invasive breast cancer cells, MMP9 mRNA and protein significantly increased, both of which were reversed by re-introducing NAT1 into the knockout cells. Following NAT1 deletion, there was an increased association of acetylated histone H3 with the SMYD3 element in the MMP9 promoter, consistent with an increase in MMP9 transcription. NAT1 deletion also up-regulated Hif1-α. Treatment of the NAT1 knockout cells with siRNA directed towards HIF1-α mRNA inhibited the increased expression of MMP9. Taken together, these results show a direct inverse relationship between NAT1 and MMP9 and suggest that HIF1-α may be essential for the regulation of MMP9 expression by NAT1.

Significance Statement:

The expression of the enzyme arylamine N-acetyltransferase 1 was found to be negatively correlated with MMP9 expression in tumor tissue from breast cancer patients. In cells, arylamine N-acetyltransferase 1 regulated MMP9 expression at a transcriptional level in a hif-1α. This finding is important as it may explain some of the pathological features associated with changes in arylamine N-acetyltransferase 1 expression in cancer.

Molecular Pharmacology Fast Forward. Published on August 23, 2019 as DOI: 10.1124/mol.119.117432
This article has not been copyedited and formatted. The final version may differ from this version.

Introduction

Arylamine N-acetyltransferase 1 (NAT1) is a xenobiotic metabolizing enzyme that catalyses the biotransformation of various carcinogens and drugs containing aromatic and heterocyclic amines (Hein, 2002). While its role in metabolism has been widely reported, recent studies have suggested that it may be important in cancer cell survival and metastasis (Butcher and Minchin, 2012; Butcher et al., 2008; Rodrigues-Lima et al., 2012). Gene deletion studies in human cancer cells have shown that NAT1 promotes invasion both *in vitro* and *in vivo* (Tiang et al., 2015). Moreover, in the absence of NAT1, cancer cells grow poorly in soft agar (Stepp et al., 2018) and can exhibit markers of mesenchymal-to-epithelial transition (Tiang et al., 2011). NAT1 has also been associated with a number of metabolic pathways including folate metabolism (Minchin, 1995), fatty acid metabolism (Carlisle et al., 2016) and the methionine salvage pathway (Witham et al., 2017). In breast cancer patients, overall survival is associated with high tumor NAT1 levels compared to low tumor NAT1 levels (Endo et al., 2014; Johansson et al., 2012; Minchin and Butcher, 2018). Moreover, there is evidence in patients that NAT1 may regulate drug resistance (Minchin and Butcher, 2018).

The family of matrix metalloproteinases (MMPs) are central to the invasive nature of many cancers. These proteases are responsible for degradation of the extracellular matrix within the vicinity of the proliferating tumor cells. This action promotes cell invasion and metastasis (Clark et al., 2008). The MMPs are secreted as latent pro-enzymes requiring activation by other proteinases (Davis et al., 2001). In breast cancer, especially triple negative breast cancer, specific MMPs have been reported to be involved in cell invasion. Of these, MMP9 has received considerable attention. MMP9 is found in more than 97% of invasive ductal carcinomas and its expression increases with histological grade (Merdad et al., 2014). Increased MMP9 expression is

negatively associated with overall survival and relapse-free survival in breast cancers (Ren et al., 2015).

MMP9 is a gelatinase that is secreted by both cancer cells and surrounding stromal cells (Noel et al., 2008). Following activation, it is involved in extracellular remodelling by degrading matrix proteins such as collagens, laminin and fibrillin. Expression of MMP9 is regulated by transcriptional and post-transcriptional processes. Recruitment of transcription factors and suppressors to the MMP9 promoter can both activate and inhibit transcription in a cell-dependent manner (Clark et al., 2008; Fanjul-Fernandez et al., 2010). Because of the observation that NAT1 inhibition decreases invasiveness, we investigated the expression of MMP9 in human breast cancer samples and in cancer cells. We found that the protease was up-regulated in highly invasive cancer cells but not in poorly invasive cells. Moreover, deletion of NAT1 gave rise to increased MMP9 expression. As this seems contrary to our previous work, we further investigated MMP9 expression to better understand the role of NAT1 in breast cancer invasion.

Materials and Methods

Materials. DMSO, puromycin and plasminogen were obtained from Sigma-Aldrich (Australia). Lomastat (GM6001) was obtained from Selleck Chemicals (USA) and gelatin fluorescein conjugate and AlexaFluor™ 647 phalloidin were obtained from Thermo Fisher Scientific (Australia). Anti- MMP9 (ab76003) was from Abcam (Canada) while anti-α-tubulin (#3873), anti-HIF1-α (#14179), anti-acetyl-histone H4K12 (#13944) and rabbit IgG (#2729) were purchased from Cell Signaling Technologies (USA). Anti-acetyl-histone H3 (#17-615) was obtained from Merck (Netherlands) while scrambled and HIF1-α siRNA (#SR320469) were from OriGene (USA).

Molecular Pharmacology Fast Forward. Published on August 23, 2019 as DOI: 10.1124/mol.119.117432
This article has not been copyedited and formatted. The final version may differ from this version.

Patient microarray data. Gene expression data were obtained through cBioPortal for Cancer Genomics (http://www.cbioportal.org). The study was also approved by the Institutional Human Ethics Committee (Approval 2017001552). All RNA levels were normalized by log(2) transformation before analysis.

Cell culture. Human breast cancer cell lines (MDA-MB-231 and T47D), human cervical cancer cell line (HeLa), human prostate cancer cell line (22Rv1) and human colon cancer cell line (HT29) were obtained from American Type Culture Collection (USA). Cancer cells were maintained in RPMI-1640 medium (Thermo Fisher Scientific) supplemented with 10% FCS (Hyclone), 2 mM L-glutamine and 100 U/ml penicillin-streptomycin (Thermo Fisher Scientific). Cells were cultured in a humidified incubator at 37°C with 5% CO_2 and passaged when they reached 80-90% confluence.

Generation of NAT1 CRISPR/Cas9 knockout cell lines. The NAT1 gene was disrupted using CRISPR/Cas9 system as previously described (Wang et al., 2018). After selection with puromycin (5 μM), single colonies were selected, expanded, and NAT1 activities measured by a high-performance liquid chromatography assay to screen for the NAT1 knockout cell lines (Butcher et al., 2000). NAT1 knockout (KO) cells were further verified by Western blot using a NAT1 specific antibody (Abcam) and PCR of genomic DNA showing NAT1 gene disruption (Wang et al., 2018).

Quantitative real-time PCR. Cells were seeded in 6-well plates at 5×10^5 cells/well and cultured for 24 hr. RNA was then extracted from cells using RNeasy Mini Kit (Invitrogen, USA) according to the manufacturer's instructions. RNA concentration and purity were measured using a NanoDrop Spectrophotometer ND-1000 (Thermo Fisher Scientific). cDNA synthesis was performed using 1.5 μg RNA and SuperScript III Reverse Transcriptase kit (Invitrogen). Each

cDNA reaction was diluted 1:5 with nuclease-free water. Quantitative real-time PCR was performed using a QuantStudio6 96-Well RT PCR system with SensiFast SYBR Green (Bioline, Australia), with the following conditions: enzyme activation at 95ºC for 10 min; denaturation at 95ºC for 10 sec, annealing at optimized temperature for 10 sec and extension at 72ºC for 20 s for 40 cycles. Target genes were amplified using specific primers (Table 1). The specificity of amplified genes was confirmed by running the PCR products on 2% agarose gels.

Gelatin degradation assay. Fluorescein-conjugated gelatin-coated coverslips were generated as previous described (Martin et al., 2012). The coated coverslips were pre-equilibrated with complete medium overnight at 37ºC before seeding cells. Cells were starved for 24 hr in medium containing 1% FCS before cell dissociation using 0.5 mM EDTA in PBS. Cells were resuspended in medium containing 10% FCS, seeded at 5×10^4 cells/well and cultured for 5.5 hr in the dark. Cells were then fixed with 4% paraformaldehyde in cytoskeletal buffer (100 mM KCl, 300 mM sucrose, 2 mM EGTA, 2 mM $MgCl_2$,10 mM PIPES, pH 7.4) for 20 min and then washed three times with PBS. Coverslips were incubated with 0.05% Triton X-100 in PBS for 5 min, washed with PBS and then blocked with 3% bovine serum albumin (BSA) in PBS for 1 hr. Phalloidin was added in 3% BSA/PBS and cells were incubated at 4ºC overnight. Coverslips were mounted with ProLong Diamond Antifade Mountant with DAPI (P36962, Thermo Fisher Scientific) and images were acquired with an Olympus FV1000 upright confocal microscope. Ten randomly selected fields were imaged per coverslip. ImageJ software was used for image analysis. Degradation area and cell number were calculated using the fluorescein-conjugated gelatin images and the phalloidin stained (F-actin) images, respectively. The relative degradation area was defined as area of degradation / cell number.

Molecular Pharmacology Fast Forward. Published on August 23, 2019 as DOI: 10.1124/mol.119.117432
This article has not been copyedited and formatted. The final version may differ from this version.

Immunoblotting. Parent, NAT1 KO and NAT1 rescue cells were seeded in 6-well plates at 5×10^5 cells/well and cultured for 24 hr. Cells were washed twice with PBS, lysed in Laemmli sample buffer and boiled at 95ºC for 5 min. Lysates were then electrophoresed at 200 V on 12% SDS-polyacrylamide gels for 45 min, transferred to nitrocellulose membranes for 1 hr at 350 mA, blocked with 5% skim milk in PBS containing 0.05% Tween-20 (PBST) for 1 hr and incubated with primary antibodies overnight at 4ºC. After three washes with PBST, membranes were incubated with horseradish peroxidase-conjugated secondary antibodies in PBST for 1 hr at room temperature. After final washes with PBST, proteins were detected using Westar ETA C 2.0 (Cyanagen, USA). Imaging was performed using a Kodak image station 4000s pro. Protein expression was quantified by densitometry using ImageJ software and normalized to α-tubulin.

Chromatin immunoprecipitation (ChIP). ChIP assays were performed using the SimpleChIP Plus Enzymatic Chromatin IP Kit (Cell Signaling) according to the manufacturer's protocol. Briefly, cells (6×10^6) were seeded in 15 cm petri dishes and cultured for 24 hr in 20 ml medium. DNA-protein crosslinking was carried out using 1% paraformaldehyde and then micrococcal nuclease was used to digest DNA to approx. 100-1000 bp. Crosslinked protein-DNA complexes were then immunoprecipitated with acetyl-histone H4K12 antibody, acetyl-histone H3 antibody or IgG (negative control). Samples (10 µl) removed before immunoprecipitation served as input controls. After reversal of cross-links and DNA purification, immunoprecipitated DNA was amplified by quantitative real-time PCR. PCRs contained 2 µl each of 0.25 µM forward and reverse primers (Table 1), 10 µl of 2× SensiFAST SYBR mix (Bioline, Australia) and 2 µl of DNA in a final volume of 20 µl. PCR was initiated by 5 min at 95°C, followed by 34 cycles of 95°C for 30 sec, 62°C for 30 sec and 72°C for 30 sec. Final extension at 72°C was for 5 min.

Molecular Pharmacology Fast Forward. Published on August 23, 2019 as DOI: 10.1124/mol.119.117432
This article has not been copyedited and formatted. The final version may differ from this version.

HIF1-α siRNA studies. Cells were seeded at 3×10^5 and cultured in 12-well plates for 48 hr. RNA-lipid complexes were prepared using Lipofectamine RNAiMAX Transfection Reagent (Thermo Fisher Scientific) according to the manufacturer's instructions. Transfected cells were cultured overnight, followed by RNA extraction for real time PCR or sample denaturation for Western blot.

Statistical analysis. Statistical analysis was performed using GraphPad Prism 7 software. Correlations of mRNA levels in breast cancer samples were determined using Spearman's correlation coefficient. Data are presented as mean ± SD. Differences in mean values between multiple groups were analyzed using one-way ANOVA. Multiple comparisons were performed using Tuckey's multiple comparisons test. P-value < 0.05 was determined as significant.

Results

Correlation between NAT1 and MMP9 expression in human cancers. To determine whether any significant correlation between NAT1 expression and MMP9 expression exists, mRNA levels were initially examined in 1904 breast cancer samples using the METABRIC dataset (Curtis et al., 2012). Figure 1A shows a negative correlation between these 2 parameters (Spearman's correlation coefficient = 0.35, $p = 5.85 \times 10^{-56}$). We have previously interrogated NAT1 expression with these data and showed the presence of 3 genetically distinct sub-populations (Minchin and Butcher, 2018). When the expression of MMP9 was assessed in each of these sub-populations (Fig. 1B), there was a clear regression with a negative slope (slope = -0.26, 95% CI = -0.29 to -0.22). This correlation was also seen in some other cancers, but not all (Table 2). There was a highly significant negative correlation also in bladder, head and neck and colorectal carcinomas whereas glioma showed the only positive correlation (p values provided in

Table 2). Taken together, these results show a negative correlation between NAT1 and MMP9 expression in at least 4 different cancers.

MMP9 expression in cancer cells following NAT1 deletion. NAT1 was deleted from 5 different cell lines using CRISPR/Cas9 technology; MDA-MB-231, T47D (breast), HT29 (colon), HeLa (cervical) and 22Rv1 (prostate). The 2 breast lines are highly invasive compared to the other lines. MMP9 expression was then quantified by qPCR (Fig. 2A). Both breast lines showed a significant increase ($p < 0.05$) in MMP9 expression, including 2 independent clones of the MDA-MB-231 cells. By contrast, there was no change in MMP9 mRNA in the 3 lines with low invasion.

To determine that the increase in MMP9 was NAT1-dependent, the MDA-MB-231 clone A was stably transfected with a NAT1 expression vector. The resulting line (rescue) had a NAT1 activity of 119.0 ± 8 nmol/min/mg protein compared to the parental line with 11.0 ± 0.2 nmol/min/mg protein. There was no detectable activity in the knockout cells. MMP9 in the rescue line was significantly less ($p = 0.001$) than that in the NAT1 knockout line (Fig. 2B). Finally, to demonstrate that the increase in MMP9 mRNA resulted in an increase in MMP9 protein, parental, knockout and rescued cells were collected and analyzed by Western blot (Fig. 2C). Both pro-MMP9 and activated MMP9 were present in the NAT1 knockout cells but not in the parental or rescue lines. These results show that NAT1 deletion causes an increase in MMP9 mRNA and protein expression that is reversed by the re-introduction of the NAT1 gene into the knockout cells.

MMP9 promoter activity following NAT1 deletion. To quantify changes in the MMP9 promoter activity following NAT1 deletion, a chromatin immunoprecipitation assay was performed to analyze histone modifications at the 3 major promoter elements of the MMP9 gene (Fig. 3A). Changes in histone acetylation have previously been shown to be associated with chromatin remodelling around the MMP9 promoter (Zhao and Benveniste, 2008; Zhong and

Kowluru, 2013). There was a significant increase ($p = 0.02$) in acetylated histone H3 associated with the SMYD3 site following NAT1 deletion but not at the proximal or distal AP-1 sites (Fig. 3B). We also examined acetylated histone H4 at each of the 3 sites, but there were no differences seen between the parental and NAT1 knockout cells (Fig. 3C). IgG isotype controls (Fig. 3D) verified the specificity of the antibodies used. When global histone acetylation was determined, there was no significant difference between parental and knockout cells (Fig. 3E). These results suggest that a localized increase in acetylated histones at the MMP9 promoter is responsible for the increase in transcription.

MMP9 up-regulation following NAT1 deletion is HIF1-α dependent. Expression of the MMPs increase under hypoxic conditions through activation of HIF1-α (Mahara et al., 2016). To assess the possible involvement of Hif1-α, its expression was quantified by Western blot in parental, NAT1 knockout and NAT1 rescue MDA-MB-231 cells. NAT1 deletion increased HIF1-α protein by 3-fold and this was restored in the rescued cells (Fig. 4A). Increased HIF1-α was not due to a change in transcription as there was no difference in mRNA levels between all 3 cell lines (Fig. 4B). Next, Hif1-α was knocked down with siRNA in the NAT1 deleted cells to investigate its involvement in MMP9 expression. Figure 4C shows the successful down-regulation of HIF1-α. Moreover, loss of HIF1-α was associated with a decrease in MMP9 mRNA (Fig. 4D), which also resulted in a decrease in pro-MMP9 and MMP9 protein (Fig. 4E). These experiments suggest up-regulation of MMP9 following NAT1 knockdown was due to elevated HIF1-α.

Up-regulation of MMP9 results in increased gelatinase activity. To examine whether the increase in MMP9 was functionally important, the ability of cells to degrade extracellular matrix proteins was assessed by culturing each cell line on fluorescently labelled gelatin. Degradation activity was determined by the increase in non-fluorescent regions beneath the attached cells (Fig.

Molecular Pharmacology Fast Forward. Published on August 23, 2019 as DOI: 10.1124/mol.119.117432
This article has not been copyedited and formatted. The final version may differ from this version.

5A). In line with the increase in MMP9, there was a significant increase ($p < 0.0001$) in gelatinase activity. Moreover, that increase was attenuated in the NAT1 rescue cells. To demonstrate that the degradation was indeed MMP-dependent, cells were treated with the MMP inhibitor GM6001. Activity in both the parental and NAT1 deleted cells was attenuated by the inhibitor (Fig. 5C). Finally, when Hif1-α was knocked down with siRNA, gelatinase activity in the NAT1 deleted cells was also attenuated (Fig. 5D), which is consistent with its role in the NAT1-dependent MMP9 expression.

Discussion

In a cohort of more than 1900 patients, there was a highly statistically significant inverse correlation between the expression of NAT1 and MMP9 in breast tumors. Breast cancer patients can be divided into 3 distinct, genetically different sub-populations according to their NAT1 mRNA levels (Minchin and Butcher, 2018). These 3 populations showed a clear difference in MMP9 expression. The negative correlation between NAT1 and MMP9 was also seen in some other cancers including bladder carcinoma and colorectal carcinoma. To investigate whether NAT1 might directly regulate MMP9 expression, several human cancer cell lines were modified using CRISPR/Cas9 to disrupt the NAT1 gene. The origin of the cells used was breast, cervical, colorectal and prostate. With the exception of the colorectal line (HT29), each cell line showed a similar effect of NAT1 on MMP9 expression to that seen in patient tumor samples (Table 2). NAT1 deletion up-regulated MMP9 transcription by more than 10-fold in the MDA-MB-231 line and this was reversed when the NAT1 gene was re-introduced into the knockout cells.

The results from the present study suggest a mechanism by which NAT1 deletion increases MMP9 expression. Low NAT1 leads to elevated HIF1-α levels, possibly through stabilizing the

protein since transcriptional changes appeared to be minimal (Fig. 4B). HIF1-α is stabilized by a number of mechanisms including acetylation at lysine 709 by p300 (Geng et al., 2012). This enzyme uses acetyl-coenzyme A, which is rate-limiting in many acetylation reactions (Pietrocola et al., 2015). Stepp *et al* reported that NAT1 deletion in human cells increases intracellular acetyl-coenzyme A levels (Stepp et al., 2018), possibly increasing HIF1-α acetylation. However, HIF1-α is also stabilized by various metabolites including pyruvate and lactate (De Saedeleer et al., 2012; Lu et al., 2002). Since NAT1 deletion inhibits mitochondrial pyruvate dehydrogenase (Wang et al., 2019), an increase in either or both of these metabolites might explain the elevated stability of HIF1-α. More work is needed to identify the exact mechanism.

In breast cancer, MMP9 is secreted by tumor cells as well as the surrounding stromal cells. MMP9 expression is associated with worse relapse-fee survival in breast (Ren et al., 2015) as well as other cancers (Huang, 2018). As a Type IV collagenase, it is capable of degrading specific proteins in the extracellular matrix. However, the role of MMP9 in cancers may not solely be related to remodelling of the tumor environment (Egeblad and Werb, 2002). For example, MMP9 can recruit inflammatory cells that enhance tumor progression (Vandooren et al., 2013). The protease also has a role in tumor angiogenesis (Vu et al., 1998) and tumor differentiation (Egeblad and Werb, 2002), both of which are associated with poor survival outcomes.

In a number of studies, NAT1 inhibition by small molecule inhibitors, shRNA or following gene deletion has been shown to induce slower cell growth (Stepp et al., 2018; Tiang et al., 2010) and decreased invasion *in vitro* (Tiang et al., 2011; Tiang et al., 2015). Moreover, NAT1 inhibition in MDA-MB-231 cells with shRNA decreased colony formation in the lungs of mice following intravenous administration. These results appear to be inconsistent with the current study where the pro-invasive MMP9 is up-regulated following NAT1 deletion. This may, in part, be related to

the diverse actions of MMP9. Moreover, NAT1 can also influence epithelial-to-mesenchymal transition (Tiang et al., 2011) and in patient tumor samples (Savci-Heijink et al., 2019). Thus, MMP9 expression alone does not predict increased invasiveness, at least not in the context of NAT1 expression.

In summary, NAT1 deletion in several cell-types results in an increase in MMP9 expression. These changes were found to be a result of higher HIF1-α levels suggesting that NAT1 may have a role in the HIF1-α pathway. Additional studies are needed to identify the exact mechanism linking these proteins in cancer as well as other pathological conditions.

Author Contributions

Participated in research design: Li, Butcher, Minchin

Conducted experiments: Li, Butcher.

Performed data analysis: Minchin, Li, Butcher

Wrote or contributed to the writing of the manuscript: Li, Butcher, Minchin

References

Butcher NJ, Ilett KF and Minchin RF (2000) Substrate-dependent regulation of human arylamine N-acetyltransferase-1 in cultured cells. *Mol Pharmacol* **57**(3): 468-473.

Butcher NJ and Minchin RF (2012) Arylamine N-acetyltransferase 1: a novel drug target in cancer development. *Pharmacol Rev* **64**(1): 147-165.

Butcher NJ, Tiang J and Minchin RF (2008) Regulation of arylamine N-acetyltransferases. *Curr Drug Metab* **9**(6): 498-504.

Carlisle SM, Trainor PJ, Yin X, Doll MA, Stepp MW, States JC, Zhang X and Hein DW (2016) Untargeted polar metabolomics of transformed MDA-MB-231 breast cancer cells expressing varying levels of human arylamine N-acetyltransferase 1. *Metabolomics :* **12**(7) pii 111.

Clark IM, Swingler TE, Sampieri CL and Edwards DR (2008) The regulation of matrix metalloproteinases and their inhibitors. *Int J Biochem Cell Biol* **40**(6-7): 1362-1378.

Curtis C, Shah SP, Chin SF, Turashvili G, Rueda OM, Dunning MJ, Speed D, Lynch AG, Samarajiwa S, Yuan Y, Graf S, Ha G, Haffari G, Bashashati A, Russell R, McKinney S, Langerod A, Green A, Provenzano E, Wishart G, Pinder S, Watson P, Markowetz F, Murphy L, Ellis I, Purushotham A, Borresen-Dale AL, Brenton JD, Tavare S, Caldas C and Aparicio S (2012) The genomic and transcriptomic architecture of 2,000 breast tumours reveals novel subgroups. *Nature* **486**(7403): 346-352.

Davis GE, Pintar Allen KA, Salazar R and Maxwell SA (2001) Matrix metalloproteinase-1 and -9 activation by plasmin regulates a novel endothelial cell-mediated mechanism of collagen gel contraction and capillary tube regression in three-dimensional collagen matrices. *J Cell Sci* **114**(Pt 5): 917-930.

De Saedeleer CJ, Copetti T, Porporato PE, Verrax J, Feron O and Sonveaux P (2012) Lactate activates HIF-1 in oxidative but not in Warburg-phenotype human tumor cells. *PLoS One* **7**(10): e46571.

Egeblad M and Werb Z (2002) New functions for the matrix metalloproteinases in cancer progression. *Nat Rev Cancer* **2**(3): 161-174.

Endo Y, Yamashita H, Takahashi S, Sato S, Yoshimoto N, Asano T, Hato Y, Dong Y, Fujii Y and Toyama T (2014) Immunohistochemical determination of the miR-1290 target arylamine N-acetyltransferase 1 (NAT1) as a prognostic biomarker in breast cancer. *Bmc Cancer* **14**.

Fanjul-Fernandez M, Folgueras AR, Cabrera S and Lopez-Otin C (2010) Matrix metalloproteinases: evolution, gene regulation and functional analysis in mouse models. *Biochim Biophys Acta* **1803**(1): 3-19.

Geng H, Liu Q, Xue C, David LL, Beer TM, Thomas GV, Dai MS and Qian DZ (2012) HIF1alpha protein stability is increased by acetylation at lysine 709. *J Biol Chem* **287**(42): 35496-35505.

Hein DW (2002) Molecular genetics and function of NAT1 and NAT2: role in aromatic amine metabolism and carcinogenesis. *Mutat Res* **506-507**: 65-77.

Huang H (2018) Matrix Metalloproteinase-9 (MMP-9) as a Cancer Biomarker and MMP-9 Biosensors: Recent Advances. *Sensors (Basel, Switzerland)* **18**(10): 3249.

Johansson I, Nilsson C, Berglund P, Lauss M, Ringnér M, Olsson H, Luts L, Sim E, Thorstensson S, Fjällskog M-L and Hedenfalk I (2012) Gene expression profiling of primary male breast cancers reveals two unique subgroups and identifies N-acetyltransferase-1 (NAT1) as a novel prognostic biomarker. *Breast Cancer Research* **14**(1): R31.

Lu H, Forbes RA and Verma A (2002) Hypoxia-inducible factor 1 activation by aerobic glycolysis implicates the Warburg effect in carcinogenesis. *J Biol Chem* **277**(26): 23111-23115.

Mahara S, Lee PL, Feng M, Tergaonkar V, Chng WJ and Yu Q (2016) HIFI-alpha activation underlies a functional switch in the paradoxical role of Ezh2/PRC2 in breast cancer. *Proc Natl Acad Sci U S A* **113**(26): E3735-3744.

Martin KH, Hayes KE, Walk EL, Ammer AG, Markwell SM and Weed SA (2012) Quantitative measurement of invadopodia-mediated extracellular matrix proteolysis in single and multicellular contexts. *J Vis Exp*(66): e4119.

Merdad A, Karim S, Schulten HJ, Dallol A, Buhmeida A, Al-Thubaity F, Gari MA, Chaudhary AG, Abuzenadah AM and Al-Qahtani MH (2014) Expression of matrix metalloproteinases (MMPs) in primary human breast cancer: MMP-9 as a potential biomarker for cancer invasion and metastasis. *Anticancer research* **34**(3): 1355-1366.

Minchin RF (1995) Acetylation of p-aminobenzoylglutamate, a folic acid catabolite, by recombinant human arylamine N-acetyltransferase and U937 cells. *Biochem J* **307 (Pt 1)**: 1-3.

Minchin RF and Butcher NJ (2018) Trimodal distribution of arylamine N-acetyltransferase 1 mRNA in breast cancer tumors: association with overall survival and drug resistance. *BMC genomics* **19**(1): 513-513.

Mittelstadt ML and Patel RC (2012) AP-1 mediated transcriptional repression of matrix metalloproteinase-9 by recruitment of histone deacetylase 1 in response to interferon beta. *PLoS One* **7**(8): e42152.

Noel A, Jost M and Maquoi E (2008) Matrix metalloproteinases at cancer tumor-host interface. *Seminars in cell & developmental biology* **19**(1): 52-60.

Pietrocola F, Galluzzi L, Bravo-San Pedro JM, Madeo F and Kroemer G (2015) Acetyl coenzyme A: a central metabolite and second messenger. *Cell metabolism* **21**(6): 805-821.

Ren F, Tang R, Zhang X, Madushi WM, Luo D, Dang Y, Li Z, Wei K and Chen G (2015) Overexpression of MMP Family Members Functions as Prognostic Biomarker for Breast Cancer Patients: A Systematic Review and Meta-Analysis. *PLoS One* **10**(8): e0135544.

Rodrigues-Lima F, Dairou J, Busi F and Dupret JM (2012) Human Arylamine N-acetyltransferase 1: From Drug Metabolism to Drug Target. *Cell Signaling & Molecular Targets in Cancer*: 23-35.

Savci-Heijink CD, Halfwerk H, Hooijer GKJ, Koster J, Horlings HM, Meijer SL and van de Vijver MJ (2019) Epithelial-to-mesenchymal transition status of primary breast carcinomas and its correlation with metastatic behavior. *Breast Cancer Res Treat* **174**(3): 649-659.

Stepp MW, Doll MA, Carlisle SM, States JC and Hein DW (2018) Genetic and small molecule inhibition of arylamine N-acetyltransferase 1 reduces anchorage-independent growth in human breast cancer cell line MDA-MB-231. *Mol Carcinog* **57**(4): 549-558.

Tiang JM, Butcher NJ, Cullinane C, Humbert PO and Minchin RF (2011) RNAi-mediated knock-down of arylamine N-acetyltransferase-1 expression induces E-cadherin up-regulation and cell-cell contact growth inhibition. *PLoS One* **6**(2): e17031.

Tiang JM, Butcher NJ and Minchin RF (2010) Small molecule inhibition of arylamine N-acetyltransferase Type I inhibits proliferation and invasiveness of MDA-MB-231 breast cancer cells. *Biochem Biophys Res Commun* **393**(1): 95-100.

Tiang JM, Butcher NJ and Minchin RF (2015) Effects of human arylamine N-acetyltransferase I knockdown in triple-negative breast cancer cell lines. *Cancer Med* **4**(4): 565-574.

Vandooren J, Van den Steen PE and Opdenakker G (2013) Biochemistry and molecular biology of gelatinase B or matrix metalloproteinase-9 (MMP-9): the next decade. *Critical reviews in biochemistry and molecular biology* **48**(3): 222-272.

Vu TH, Shipley JM, Bergers G, Berger JE, Helms JA, Hanahan D, Shapiro SD, Senior RM and Werb Z (1998) MMP-9/gelatinase B is a key regulator of growth plate angiogenesis and apoptosis of hypertrophic chondrocytes. *Cell* **93**(3): 411-422.

Wang L, Minchin RF and Butcher NJ (2018) Arylamine N-acetyltransferase 1 protects against reactive oxygen species during glucose starvation: Role in the regulation of p53 stability. *PLoS One* **13**(3): e0193560.

Wang L, Minchin RF, Essebier PJ and Butcher NJ (2019) Loss of human arylamine N-acetyltransferase I regulates mitochondrial function by inhibition of the pyruvate dehydrogenase complex. *Int J Biochem Cell Biol* **110**: 84-90.

Witham KL, Minchin RF and Butcher NJ (2017) Role for human arylamine N-acetyltransferase 1 in the methionine salvage pathway. *Biochem Pharmacol* **125**: 93-100.

Zhao X and Benveniste EN (2008) Transcriptional activation of human matrix metalloproteinase-9 gene expression by multiple co-activators. *Journal of molecular biology* **383**(5): 945-956.

Zhong Q and Kowluru RA (2013) Regulation of matrix metalloproteinase-9 by epigenetic modifications and the development of diabetic retinopathy. *Diabetes* **62**(7): 2559-2568.

Footnotes

This work was funded by the National Health and Medical Research Council of Australia (Grant number 1083036. Pengcheng Li was supported by the CSC-UQ PhD Scholarship program. Results published here are based upon data generated by the METABRIC consortium (http://molonc.bccrc.ca/aparicio-lab/research/metabric/). The authors acknowledge the contributions made by the organizers of the databases and donors of samples used in the present study.

Molecular Pharmacology Fast Forward. Published on August 23, 2019 as DOI: 10.1124/mol.119.117432
This article has not been copyedited and formatted. The final version may differ from this version.

Figure Legends

Fig. 1. Correlation between NAT1 and MMP9 mRNA levels in breast tumors. (A) mRNA levels in 1904 patient samples were plotted and correlation was estimated using Spearman's correlation coefficient (rho = 0.35, $p = 5.85 \times 10^{-56}$). Solid line is the estimated regression. (B) The regression of NAT1 and MMP9 was determined in 3 genetically distinct NAT1 sub-populations (Minchin and Butcher, 2018). For the lowest NAT1 population (n = 447), NAT1 mRNA varied from 5 to 6.5 (log2 scale) whereas for the intermediate population (n = 382), it varied from 7.25 to 8.5. In those patients with highest NAT1 (n = 558), mRNA varied from 10 to 13. Data are mean ± SD.

Fig. 2. Expression of MMP9 in cancer cells following NAT1 deletion. (A) MMP9 mRNA was quantified by qPCR in high invasive (MDA-MB-231 (231) clone A and B, T47D) and low invasive (HT29, HeLa, 22Rv1) cells. Solid bars = parental cells; open bars = NAT1 deleted cells. Data are normalized to actin and expressed relative to the parental cells as mean ± SD, n = 3. Asterisk = $p < 0.05$. (B) Restoration of MMP9 expression in MDA-MB-231 NAT1 rescued (RE) cells compared to parental (P) and NAT1 deleted (KO) cells. (C) Expression of pro-MMP9 and MMP9 protein in the parental, NAT1 knockout and NAT1 rescue MDA-MB-231 cells.

Fig. 3. Chromatin immunoprecipitation (ChIP) assay for acetylated histone associated with the MMP9 promoter. (A) Schematic of the MMP9 promoter highlighting the 3 major transcription factor binding sites. Adapted from (Mittelstadt and Patel, 2012). The PCR fragments for the proximal AP-1, distal AP-1 and SMYD3 sites are shown by arrows. (B) Fold enrichment of each site in the ChIP assay relative to parental MDA-MB-231 cells using anti-acetylated histone H3 antibody for immunoprecipitation. (C) Fold enrichment of each site in the ChIP assay relative to

parental cells using anti-acetylated histone H4K12 antibody for immunoprecipitation. (D) ChIP assay using IgGisotype control demonstrating minimal non-specific effects. (E) Global acetylated histone H3 (H3) and histone H4K12 (H4K12) in MDA-MB-231 parental and NAT1 knockout cells. All results are mean ± SD, asterisk = $p < 0.05$, n = 3. P = parental cells, KO = knockout cells.

Fig. 4. Effect of NAT1 deletion on HIF1-α and MMP9 expression. (A) HIF1-α protein in MDA-MB-231 parental (P), NAT1 knockout (KO) and NAT1 rescue (RE) cells. (B) Effect of NAT1 deletion on HIF1-α mRNA. (C) siRNA knockdown of HIF1-α in NAT1 deleted cells. Scr = scrambled siRNA, siHIF = Hif1-α targeted siRNA. (D) Effect of Hif1-α knockdown with siRNA on MMP9 mRNA in NAT1 deleted cells. (E) Effect of Hif1-α knockdown with siRNA on MMP9 protein in NAT1 deleted cells. All results are mean ± SD, asterisk = $p < 0.05$, n = 3.

Fig. 5. Gelatin degradation assay following NAT1 deletion. (A) Representative confocal images of parental (P), NAT1 knockout (KO) and NAT1 rescue (RE) MDA-MB-231 cells grown on fluorescein conjugated gelatin coated coverslips (green) after 5.5 hr incubation. Cells were also stained with phalloidin (F-actin, red). White arrows indicate regions of gelatin degradation. (B) Quantification of gelatin degradation capacity for MDA-MB-231 cells. (C) Effect of 20 μM GM6001 on gelatin degradation. (D) Effect of Hif1-α knockdown with siRNA on the gelatin degradation by parental (P) and NAT1 knockout (KO) cells. Scr = scrambled siRNA, siHif = Hif1-α targeted siRNA. Data are means ±SD, $N \geqslant 18$. Asterisk = $p < 0.05$.

Molecular Pharmacology Fast Forward. Published on August 23, 2019 as DOI: 10.1124/mol.119.117432
This article has not been copyedited and formatted. The final version may differ from this version.

Tables

TABLE 1.

List of oligonucleotides used for real time PCR and ChIP assays

Primer	**Forward (5'- to -3')**	**Reverse (5'- to -3')**
β-Actin	CCTCGCCTTTGCCGATCC	GGATCTTCATGAGGTAGTCAGTC
MMP9	GCACGACGTCTTCCAGTACC	GCACTGCAGGATGTCATAGGT
MMP9 AP1 (distal)	CTTGCCTAGCAGAGCCCATT	TTTTTCCCTCCCTGACAGCC
MMP9 AP1 (proximal)	AGAGAGGAGGAGGTGGTGTAAGC	ACCCCACCCCTCCTTGAC
MMP9 SMYD3	GGGATCCCTCCAGCTTCATC	GGTTTTGCAAACTGCAGAGCTT
HIF1-α	GCCGCTGGAGACACAATCAT	GAAGTGGCTTTGGCGTTTCA

Molecular Pharmacology Fast Forward. Published on August 23, 2019 as DOI: 10.1124/mol.119.117432
This article has not been copyedited and formatted. The final version may differ from this version.

TABLE 2.

Correlation between NAT1 and MMP9 expression in human cancers.

Data extracted from cBioPortal and analyzed using online tools available at the database site (http://www.cbioportal.org/). N = # patients, rho = Spearman's correlation coefficient. p = probability, ns = not significant.

Tumor	Database	N	rho	p
Breast invasive carcinoma	METABRIC	1904	-0.350	$<10^{-55}$
Breast invasive carcinoma	TCGA PanCancer Atlas	994	-0.272	$<10^{-17}$
Bladder urethral carcinoma	TCGA PanCancer Atlas	406	-0.255	$< 10^{-6}$
Head and neck squamous cell carcinoma	TCGA PanCancer Atlas	438	-0.263	$< 10^{-5}$
Colorectal adenocarcinoma	TCGA PanCancer Atlas	640	-0.176	$<10^{-4}$
Glioblastoma multiforme	TCGA PanCancer Atlas	145	0.124	ns
Cervical squamous cell carcinoma	TCGA PanCancer Atlas	275	-0.108	ns
Stomach adenocarcinoma	TCGA PanCancer Atlas	407	-0.032	ns
Lung adenocarcinoma	TCGA PanCancer Atlas	503	-0.003	ns
Lung squamous cell carcinoma	TCGA PanCancer Atlas	466	0.055	ns
Ovarian cystadenocarcinoma	TCGA PanCancer Atlas	201	0.079	ns
Prostate adenocarcinoma	TCGA PanCancer Atlas	487	0.069	ns
Cutaneous melanoma	TCGA PanCancer Atlas	363	0.052	ns
Thyroid carcinoma	TCGA PanCancer Atlas	480	-0.001	ns
Endometrial carcinoma	TCGA PanCancer Atlas	507	0.010	ns
Glioma (low grade)	TCGA PanCancer Atlas	507	0.314	$< 10^{-12}$

Figure 1

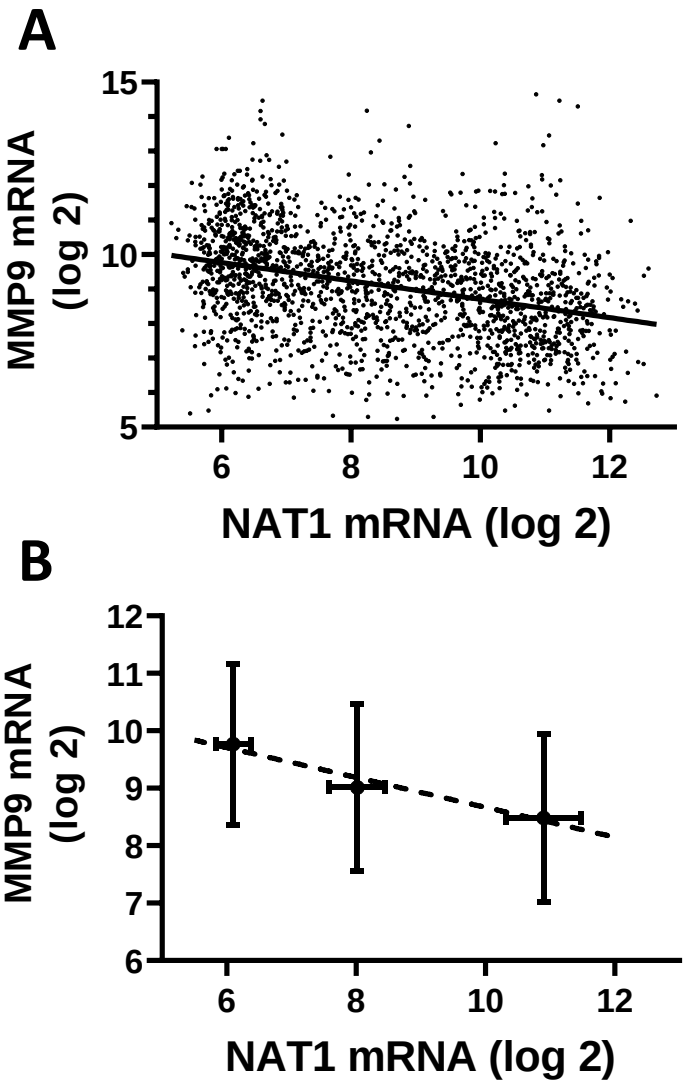

Figure 2

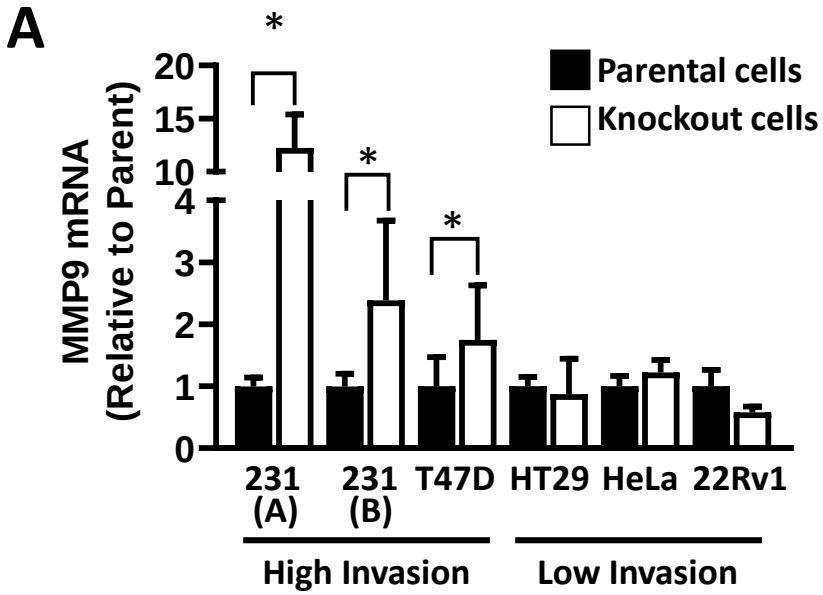

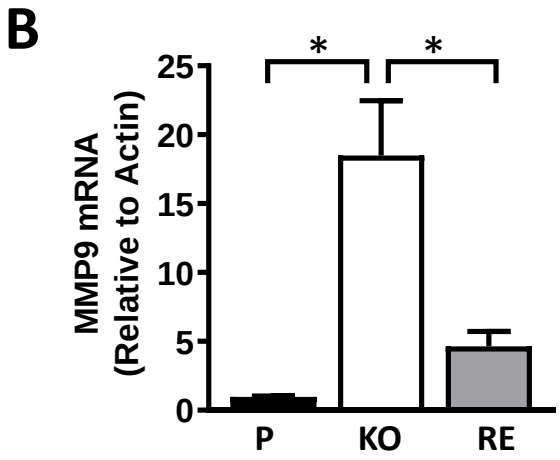

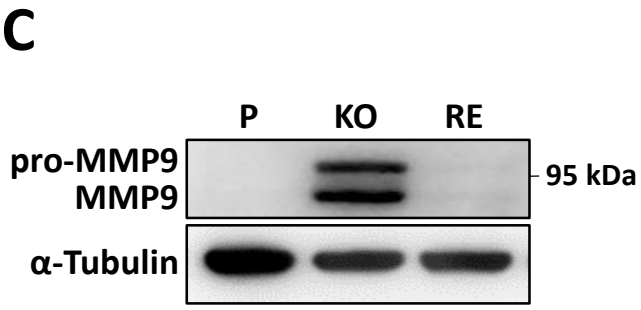

Molecular Pharmacology Fast Forward. Published on August 23, 2019 as DOI: 10.1124/mol.119.117432
This article has not been copyedited and formatted. The final version may differ from this version.

Figure 3

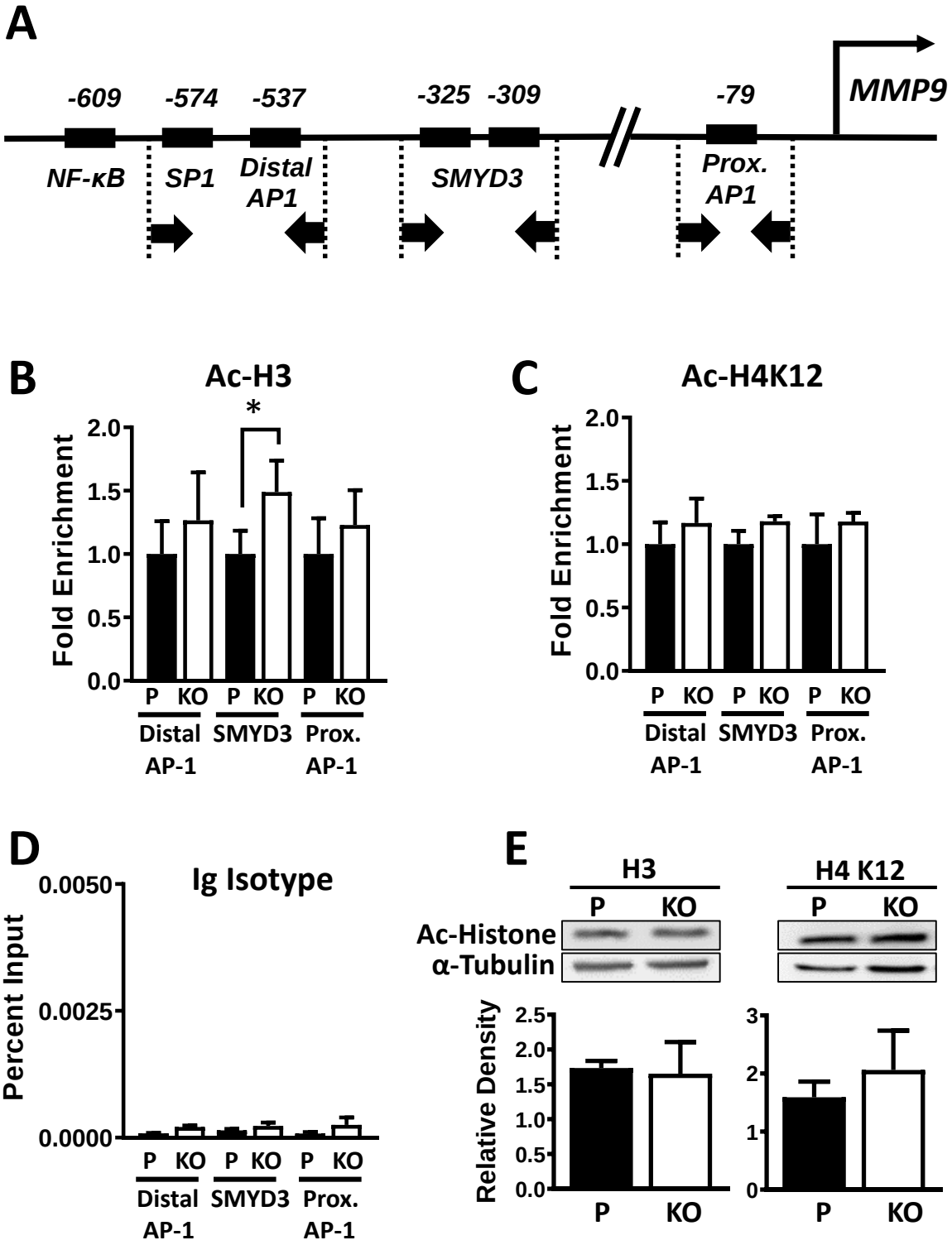

Molecular Pharmacology Fast Forward. Published on August 23, 2019 as DOI: 10.1124/mol.119.117432
This article has not been copyedited and formatted. The final version may differ from this version.

Figure 4

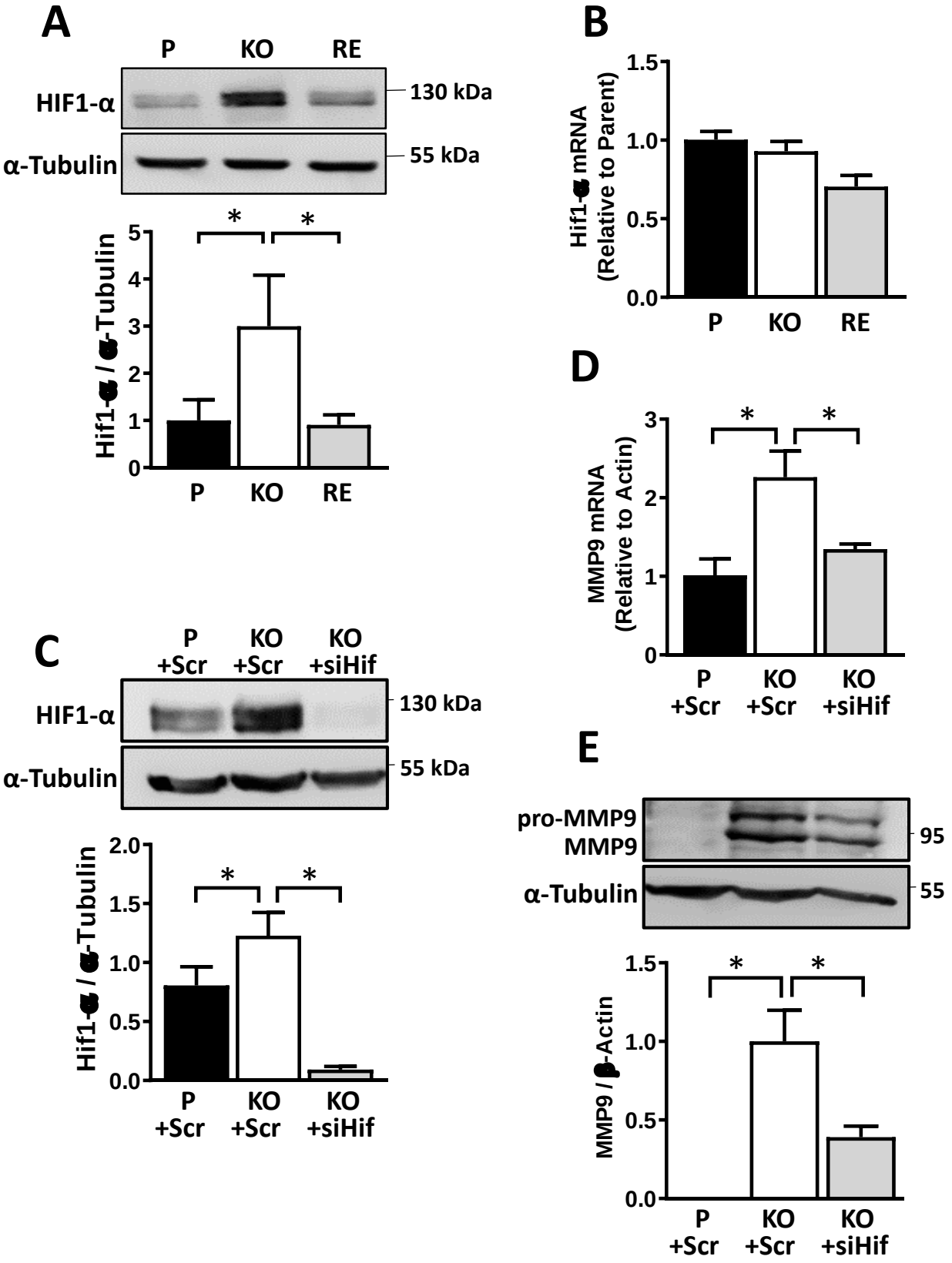

Molecular Pharmacology Fast Forward. Published on August 23, 2019 as DOI: 10.1124/mol.119.117432
This article has not been copyedited and formatted. The final version may differ from this version.

Figure 5